Journal of Alloys and Compounds 834 (2020) 155063

Contents lists available at ScienceDirect

Journal of Alloys and Compounds

journal homepage: http://www.elsevier.com/locate/jalcom

Effects of nitrogen content on microstructures and mechanical properties of (AlCrTiZrHf)N high-entropy alloy nitride films

Panpan Cui [a], Wei Li [a, *], Ping Liu [a], Ke Zhang [a], Fengcang Ma [a], Xiaohong Chen [a], Rui Feng [b], Peter K. Liaw [b]

[a] School of Materials Science and Engineering, University of Shanghai for Science and Technology, Shanghai, 200093, PR China
[b] Department of Materials Science and Engineering, The University of Tennessee, Knoxville, TN, 37996, USA

ARTICLE INFO

Article history:
Received 12 November 2019
Received in revised form
3 April 2020
Accepted 4 April 2020
Available online 9 April 2020

Keywords:
(AlCrTiZrHf)N high-Entropy alloy nitride films
Magnetron sputtering
Nitrogen content
Microstructure
Mechanical properties

ABSTRACT

The (AlCrTiZrHf)N high-entropy alloy nitride films were synthesized by reactive magnetron sputtering. The effects of different N_2 flow rates on the microstructures and mechanical properties of (AlCrTiZrHf)N films were studied by the X-ray diffraction (XRD), scanning electron microscopy (SEM), high-resolution transmission electron microscopy (HRTEM), nanoindentation, coating friction and wear tester. The results show that the AlCrTiZrHf high-entropy alloy film presents an amorphous state. With the increase of the N_2 flow rate, the (AlCrTiZrHf)N high-entropy alloy nitride films transform to a face-centered-cubic (FCC) structure. When the N_2:Ar ratio is 5:4, the hardness and elastic modulus of the films reach 33.1 GPa and 347.3 GPa, respectively. The strengthening effect is mainly attributed to the formation of saturated metal-nitride phases and the solid-solution strengthening of various elements. Meanwhile, the (AlCrTiZrHf)N film exhibits the low friction coefficient and superior wear resistance. Based on the excellent properties of high-entropy alloy nitride films, the (AlCrTiZrHf)N film presents a potential application in protective coating.

1. Introduction

With the rapid development of the machining industry, the performance requirements for hard film/coating materials are becoming higher and higher. The traditional binary and ternary coatings, such as TiN [1], CrN [2] and TiAlN [3], can no longer meet the increasingly demanding working environment. Due to the high hardness, high strength, high wear resistance and high ultimate tensile strength of high-entropy alloy nitride films [4–9], more and more scholars have been interested in the research of high-entropy alloy nitride films in recent years.

Compared with traditional alloys, high-entropy alloys are also called multi-principal element alloys, which are composed of five or more metal elements or non-metal elements in equal or near-equal atomic ratios [10]. The so-called high-entropy alloy (HEA) or equiatomic multicomponent alloy was innovatively proposed in 2004 by Yeh and Cantor, respectively, who broke through the traditional concept of alloys [11–14]. Due to the high-entropy effect, the high-entropy alloy not only does not form a large number of intermetallic compounds after solidification, but present a simple face-centered-cubic (FCC) or body-centered-cubic (BCC) crystalline phase [15,16], or two phases in common alloys, such as eutectic high-entropy alloys (EHEA) [17,18].

In recent years, more and more attention has been paid to the high-entropy alloy nitride films due to attractive mechanical properties. Sha et al. [19] prepared the nitride films of FeMnNiCoCr by direct current (DC) magnetron sputtering. It was found that as the nitrogen flow rate increased, the nitrogen flow rate enhanced the self-organizing behavior of the metal atoms, leading to the transition of the high-entropy alloy (FeMnNiCoCr)N_x film from the FCC to BCC structure. At high nitrogen contents (~26 at. %), The film exhibited excellent hardness, abrasion resistance, and good scratch response. Ren et al. [20] prepared (VAlTiCrMo)N_x high-entropy alloy nitride coating, which not only enhanced the mechanical properties with the introduction of nitrogen, but also improved the corrosion resistance of the nitride coating in a 3.5 wt.% NaCl solution. In the investigation on Al–Cr–Nb–Y–Zr–N films prepared by Fieandt et al. [21], some nano-level element segregation was found in all the samples, and the films showed different segregation behaviors depending on the nitrogen content. The hardness of the film increased with increasing the nitrogen content, and at a nitrogen content of 50 at. %, the hardness reached the maximum

* Corresponding author. School of Materials Science and Engineering, University of Shanghai for Science and Technology, Shanghai, 200093, China.
E-mail address: liwei176@usst.edu.cn (W. Li).

https://doi.org/10.1016/j.jallcom.2020.155063
0925-8388/

value of 30 GPa). Feng et al. [22] investigated the effect of various $N_2/(Ar + N_2)$ flow ratios (R_N) on the multi-element CrTaNbMoV nitride films. The results showed that the nitride films deposited at $R_N = 20\%$ presented the highest hardness and critical load (Lc). At this time, the wear rate of the film was six times lower than that of the alloy film, indicating an excellent wear resistance.

Transition elements are the main elements commonly used in HEAs. Al, Cr, Ti, and Zr, are all strong nitride-forming elements. These elements can combine with N elements to form films with higher mechanical properties [23–26]. Hf can inhibit grain-boundary coarsening, strengthen grain boundaries, increase the hardness and elastic modulus of the film, and significantly reduce the content of solid-solution micropores [27]. Moreover, the Hf element can easily react with N to form HfN with an FCC structure [28]. Therefore, a high-entropy alloy nitride film composed of Al–Cr–Ti–Zr-Hf elements is expected to present good mechanical properties. However, relevant report on the (AlCrTiZrHf)N film has been rarely documented. To this end, the (AlCrTiZrHf)N films with different nitrogen contents are synthesized by reactive magnetron sputtering in this investigation. The effect of nitrogen content on the microstructures and mechanical properties of (AlCrTiZrHf)N film are studied, which expects to provide research support for its industrial application.

2. Experimental

2.1. Film preparation

The (AlCrTiZrHf)N films were deposited on single-crystal silicon wafers by the equal-moles AlCrTiZrHf target (99.99%, volume percent) in a JGP-450 multi-target magnetron sputtering system. The target size was 75 mm in diameter and 3 mm in thickness, and the single-crystal silicon wafer size was 30 mm × 20 mm x 0.5 mm. Before the deposition, the silicon wafer was cleaned by ethanol and acetone in the ultrasonic-cleaning machine with frequencies of 30–80 kHz, respectively, for 10–15 min before drying. When the vacuum in the sputtering chamber was less than 3×10^{-3} Pa, a mixture of high purity nitrogen and argon (99.99%) (N_2:Ar = 0:4, 2:4, 3:4, 4:4, 5:4, and 6:4) was introduced into the sputtering chamber for reactive sputtering in order to obtain a high-entropy alloy film with different nitrogen contents. The target was controlled by a radio frequency (R.F.) power source, and the sputtering power was 300 W. The working pressure was 3×10^{-3} Pa with the deposition time of 2 h. The silicon wafer was not heated during the deposition process.

2.2. Film characterization and measurement

The phase composition of (AlCrTiZrHf)N films were analyzed by the D8 Advance X-ray diffractometer (XRD, Bruker, Germany) using the CuK_α radiation ($\lambda = 0.15406$ nm) with a measurement range of 10°–90°. The microstructures of the films were observed by the Quanta FEG450 field emission environmental electron microscope (SEM, FEI, USA) and Tecnai $G^2$20 high-resolution field-emission transmission electron microscope (HRTEM, FEI, USA). The elemental distributions of the films were characterized by the electron probe microanalyzer (EPMA, JXA-8530F PLUS). The hardness of the film was measured by a NANO Indenter G200 nano-indenter (Agilent, USA) with the Berkovich indenter. The load-unload curve was obtained by accurately recording the change of the indentation depth with load. The hardness of the material was calculated by the Oliver-Pharr model [29]. The depth of penetration was less than 1/10 of the thickness of the film in order to eliminate the effect of the substrate on the hardness of the film. The friction coefficient of the film was measured by the HRS-2M high-speed friction and wear tester. The friction pair was a GCr15 steel ball of a diameter, d = 4 mm. The applied load was 8 N, and the test time was 3 min.

3. Results

3.1. Effect of the N_2 flow rate on the film deposition rate and composition

Fig. 1 shows the sputtering rate of (AlCrTiZrHf)N high-entropy alloy nitride film. It can be seen that the sputtering rate of the film sharply reduces from 25.57 nm/min to 11.03 nm/min after N_2 is introduced. As the N_2 flow continues to increase, the sputtering rate continues to decrease. The main reason for the decrease of the sputtering rate is that the high nitrogen flow rate will lead to target poisoning, which will reduce the deposition rate of the films [30–33].

Fig. 2 shows that when no nitrogen is introduced, the contents of five metal elements in AlCrTiZrHf high-entropy alloy films are between 17.48 at. % - 21.16 at. % (atomic percentage). The difference in the content of each element is due to the different sputtering yields of Ar^+ ions on each metal element. With the increase of the N_2 flow rate, the nitrogen content in high-entropy alloy films increases rapidly at first and then stabilizes. When the N_2:Ar ratio is 3:4, the nitrogen content in the film tends to be stable, which is about 50 at.%. This trend can be due to the fact that the high-entropy alloy film tends to form a solid-solution phase composed of metal nitrides as the flow rate of N_2 increases. When the nitrogen content continues to increase, the N atom will dissolve into the lattice of the high-entropy alloy nitride film. Therefore, the nitrogen content of the high-entropy alloy film increases slightly when the N_2:Ar ratio is greater than 1:1. Since the bond energy between the metal and the nitrogen is greater than the bond energy between the metal and the metal [34], the metal atom preferentially combines with the nitrogen atom to form the metal nitride. As a result, the atomic percentage of nitrogen to metal element tends to be 1:1.

3.2. Effect of the N_2 flow rate on microstructures

Fig. 3 shows the XRD patterns of (AlCrTiZrHf)N high-entropy alloys nitride films with different N_2 flow rates. When the nitrogen flow rate is 0, the XRD pattern of AlCrTiZrHf film presents a

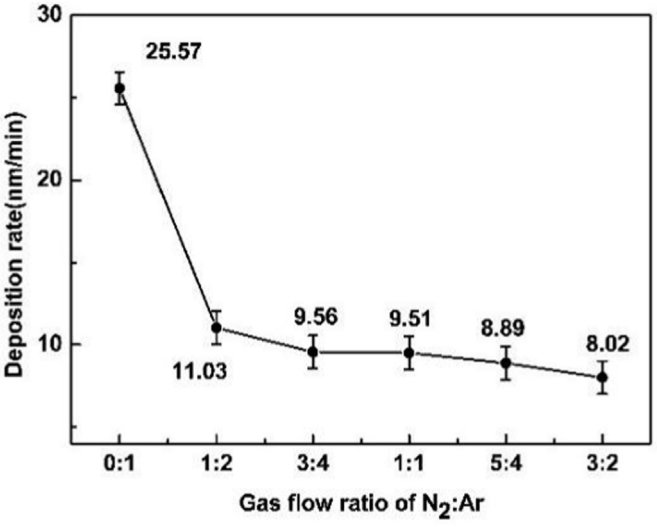

Fig. 1. Sputtering rate of (AlCrTiZrHf)N high-entropy alloy nitride film.

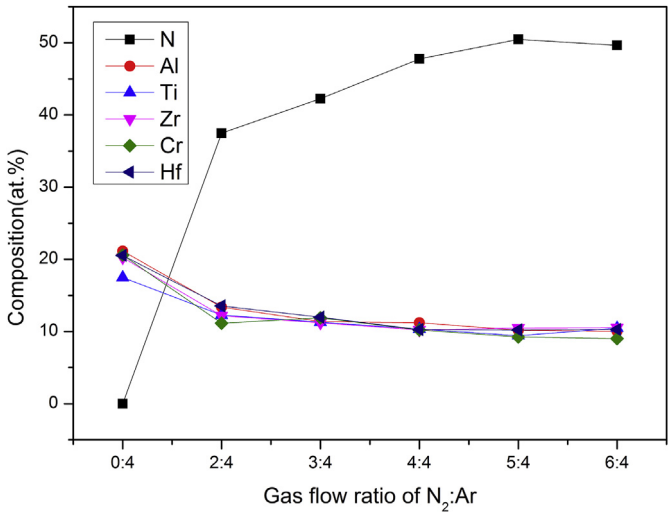

Fig. 2. EPMA element contents in (AlCrTiZrHf)N coatings deposited at various gas flow ratios of N_2:Ar.

wide peak. The crystallinity of the AlCrTiZrHf high-entropy alloy film is weak, showing an amorphous state. The high mixing entropy and the large atomic-size difference are the main reasons for the formation of an amorphous state [35].

With the introduction of N_2, the crystallinity of the film increases, and the (111) and (220) diffraction peaks appear in the (AlCrTiZrHf)N high-entropy alloy nitride film, manifesting the preferential growth of the (111) crystal plane, which indicates that the (AlCrTiZrHf)N film is composed of an FCC-structured solid-solution phase. The main reason for the formation of the solid solution is that the high-entropy effect increases the solid solubility between the elements and inhibits the formation of intermetallic compounds between the metal element and the nitrogen [36]. The high-entropy effect enhances the mutual solubility of the target metal elements and slows long-distance diffusion, helping maintain a solid solution [11,30].

In addition, the lattice constant of the nitride coating has the same tendency as the nitrogen content [36]. When the nitrogen content is higher than 50 at. %. The coating has formed a nitride coating with an excess stoichiometric ratio. The element N exists in the interstitial solid solution as an atomic state, resulting in an increase in the lattice constant of the nitride coating.

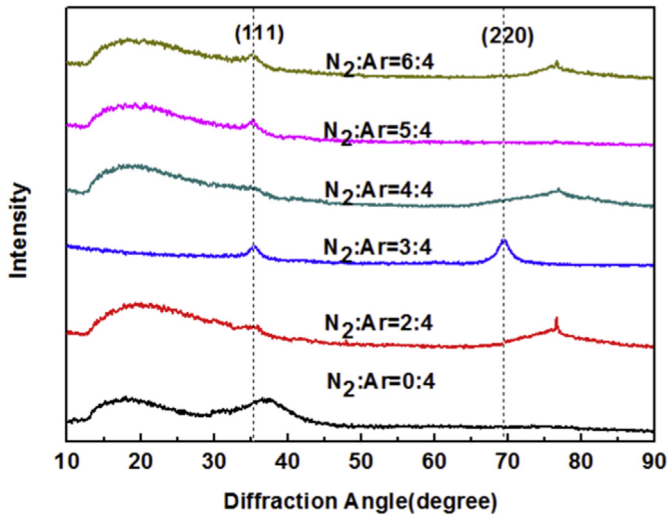

Fig. 3. XRD patterns of (AlCrTiZrHf)N high-entropy alloy nitride films with different N_2 flow rates.

Fig. 4 is the cross-sectional SEM images of the (AlCrTiZrHf)N high-entropy alloy nitride film. As presented in the figures, the films have the uniform thickness and smooth surface. No obvious surface or internal defects can be detected. When the N_2 flow rate is 0, no visible grain characteristics are observed in the cross-sectional fracture of the film. As the flow rate of N_2 increases, the thickness of the film gradually decreases, mainly attributed to the drop of the sputtering rate. With the increase of the N_2 flow, the film may change from the amorphous to crystalline phase due to the formation of a nitride structure. It can also be seen from Fig. 3 that the cross-sectional fracture of the (AlCrTiZrHf)N film is smooth, and the obvious columnar crystals can be seen.

The cross-sectional HRTEM morphology of the (AlCrTiZrHf)N high-entropy alloy nitride film with the N_2:Ar ratio of 5:4 are presented in Fig. 5. From Fig. 5(a), it can be seen that there are many fine nanocrystals in the films. The uniform texture of the films shows a single solid-solution phase, which can be explained from the fact that the high-entropy effect makes the films homogenize the microstructures and tend to form nanocrystalline and amorphous phases [37]. Moreover, the high-entropy effect and hysteretic-diffusion effect [38] help inhibit the precipitation of metal compounds, so that the high-entropy alloy film has a single-phase solid-solution structure. From the selected area electron diffraction patterns, the (111), (200), and (220) crystal planes can be observed, indicating the FCC structure of the (AlCrTiZrHf)N film, which is in accordance with the XRD results in Fig. 3. The columnar crystal-growth orientation of the film is shown by the arrow in Fig. 5(b).

3.3. *Effect of the N_2 flow rate on mechanical properties*

Fig. 6 shows the hardness and elastic modulus of (AlCrTiZrHf)N high-entropy alloy nitride films with the different N_2 flow rates. It can be seen that, with the increase of the nitrogen flow rate, the hardness and elastic modulus of the films increase from 17.9 GPa to 33.1 GPa and 262.3 GPa—347.3 GPa, respectively. Compared with the AlCrTiZrHf alloy film, the hardnesses and elastic moduli of the films significantly increase. When N_2:Ar = 5:4, the hardness of the film rises up to 33.1 GPa, and the N content in the film also reaches a maximum of 50.48 at.%. The increase of hardness is mainly attributed to the formation of saturated metal nitride phases and the solid-solution strengthening of various elements. As the N content continues to increase, the excess N element will form the nitride on the surface of the alloy target, thereby causing reactive sputtering of the film to convert into direct sputtering of the nitride, resulting in the decreases of hardness and elastic modulus.

Fig. 7 shows the friction coefficients of the (AlCrTiZrHf)N high-entropy alloy nitride films with different N_2 flow rates. The friction coefficient of the AlCrTiZrHf alloy film is 0.65. With the increase of the nitrogen flow rate, the friction coefficient of the high-entropy alloy-nitride film first decreases and then increases. When the nitrogen-argon flow rate is 5:4, the friction coefficient of the high-entropy alloy nitride film reaches the lowest value of 0.5. As the N_2 flow rate continues to increase, the nitrogen atom content is too high and the amount of metal-nitride phases in the film increases rapidly. The above trend results in the formation of the defects, such as columnar coarse crystals and pores, which leads to the decrease in the hardness and elastic modulus of the film and increase in the friction coefficient.

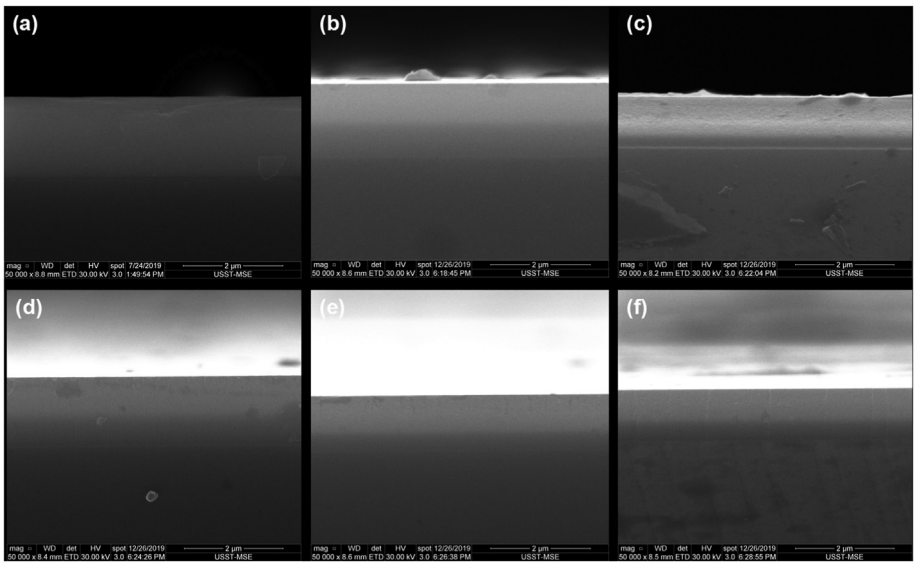

Fig. 4. Cross-sectional SEM morphology of the (AlCrTiZrHf)N high-entropy alloy nitride film: (a) N_2:Ar = 0:4; (b) N_2:Ar = 2:4; (c) N_2:Ar = 3:4; (d) N_2:Ar = 4:4; (e) N_2:Ar = 5:4; and (f) N_2:Ar = 6:4.

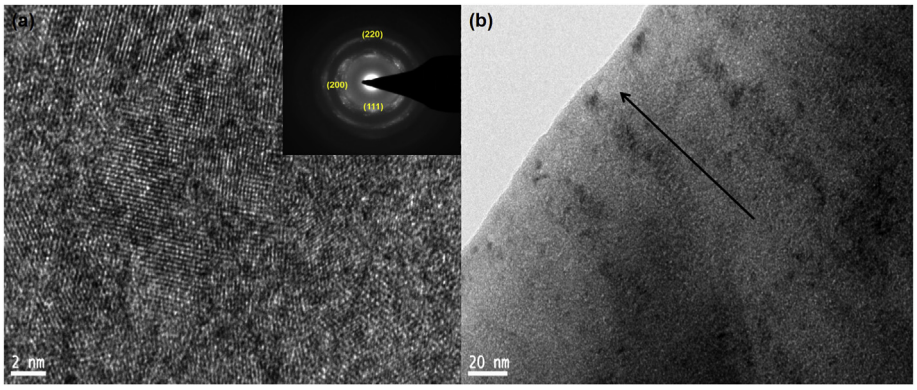

Fig. 5. Cross-sectional HRTEM morphology of the (AlCrTiZrHf)N high-entropy alloy nitride film with the N_2:Ar ratio of 5:4: (a) high magnification and selected area electron diffraction pattern (b) low magnification.

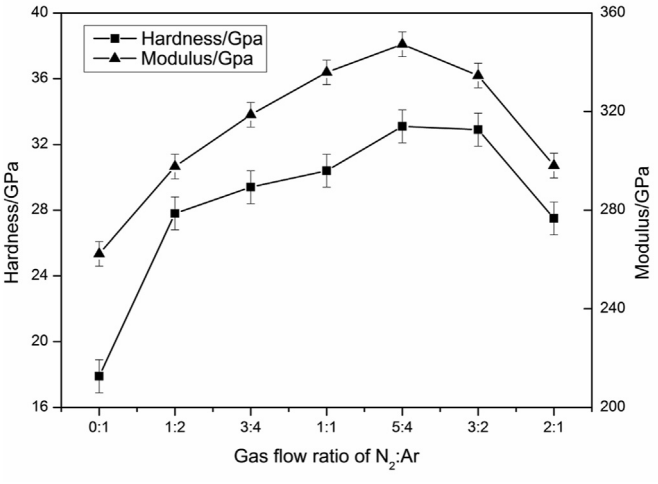

Fig. 6. Hardnesses and elastic moduli of (AlCrTiZrHf)N high-entropy alloy nitride films with different N_2 flow rates.

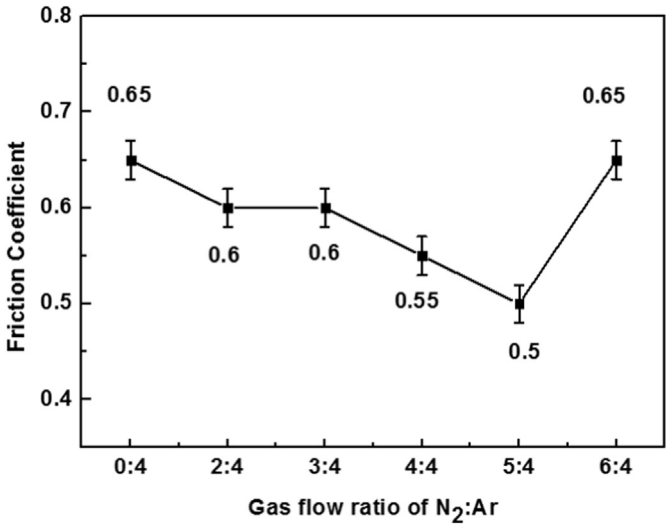

Fig. 7. Friction coefficients of (AlCrTiZrHf)N high-entropy alloy nitride films with different N_2 flow rates.

4. Discussion

4.1. Influence of the N content on microstructures of films

High-entropy alloy films exhibit an amorphous structure due to their high mixing entropy and large atomic-size difference. The high mixing entropy increases the mutual solubility between the constituent metal elements, and the large atomic-size difference leads to the lattice distortion to form an amorphous phase structure. This phenomenon is consistent with previous studies on multi-element films, such as TiVCrZrAl [39], AlCrTaTiZr [40], AlCrMoSiTi [32], AlCrNiSiTi [41], and AlCrSiTiV [42]. With the introduction of N_2, the crystallinity of the film increases, the (AlCrTiZrHf)N high-entropy alloy nitride film gradually forms an FCC-structured solid-solution phase. The structures of the binary nitrides of Cr, Ti, Zr, and Hf are all FCC, while the AlN structure is hexagonal-close-packed (HCP). Therefore, the FCC structure dominates the crystal structure due to the high-entropy effect, which is similar to a massive high-entropy alloy in which the high mixing entropy enhances the formation of a solid-solution phase [30]. Previous reports describe similar observations of other multi-element nitrides [40,43,44].

Through the SEM image of the (AlCrTiZrHf)N high-entropy alloy nitride film, the columnar crystal structure can be clearly observed at the fracture of the (AlCrTiZrHf)N high-entropy alloy-nitride films. This phenomenon is considered to be the result of recombination and recrystallization when the N_2 flow rate is relatively high [36]. Because of the different anisotropic growth rates, some grains tend to overgrow other grains, thus forming a columnar structure. According to the HRTEM image of the (AlCrTiZrHf)N high-entropy alloy-nitride film, it can be observed that many fine nanocrystals are distributed in the film, and the film has a uniform texture and presents a single solid-solution phase. Combined with the selected area electron diffraction pattern, it can be confirmed that the (AlCrTiZrHf)N high-entropy alloy nitride film presents the FCC structure.

4.2. The improvement of mechanical properties

Compared with the high-entropy alloy film without N_2, the hardness and elastic modulus of the (AlCrTiZrHf)N high-entropy alloy nitride film significantly increase with the addition of N_2, mainly explained by the fact that the content of N in the films rapidly increases after N_2 is introduced. The above trend can be due to the fact that the bonding bond of Me—N is much stronger than that of Me-Me [34]. The rapid increase of the N content leads to the formation of the saturated ceramics phase of the nitride in the films. Therefore, the hardnesses and elastic moduli of the films greatly increase.

Since the (AlCrTiZrHf)N high-entropy alloy nitride film is actually a solid solution of five binary nitrides, there are large differences in the atomic size among the five target elements. It also provides a strong solid-solution strengthening effect due to the combination of polyatomic components of different atomic sizes [30,34]. Therefore, the hardness of the (AlCrTiZrHf)N high-entropy alloy nitride film is significantly higher than that of the AlCrTiZrHf high-entropy alloy film.

However, as the N content continues to increase, the film hardness and elastic modulus do not increase, but decrease. The main reason for this phenomenon is that an excessive amount of N elements causes a nitride to form on the surface of the alloy target, thereby making reactive sputtering of the film convert into direct sputtering of the nitride. This transformation not only results in a decrease in the sputtering rate of the film, but also leads to a decrease in the quality of the film, which in turn causes a slight decrease in the hardness and elastic modulus of the (AlCrTiZrHf)N film, as shown in Fig. 6.

According to Archard's law [45]:

$$V = K \cdot \frac{N \cdot L}{H} \tag{1}$$

where K is the wear coefficient, L is the sliding stroke, N is the load, and H is the hardness. The wear rate is inversely proportional to the hardness of the alloy. In the above analysis, since the hardness of the high-entropy alloy film is increased due to the formation of the nitride-ceramic phase in the film, the film wear rate is lowered. However, compared with the high-entropy alloy film without N_2, the friction coefficient of the (AlCrTiZrHf)N high-entropy alloy nitride film is reduced due to the formation of the saturated nitride ceramic phase in the film. The nitride-ceramic phase has the characteristics of the high hardness, great high wear resistance, and low friction coefficient [46]. Therefore, the reduction of the friction coefficient is mainly due to the formation of the nitride-ceramic phase. Similarly, if the N-atom content is too high, defects in the film will cause a decrease in the hardness and elastic modulus, resulting in an increase in the friction coefficient of the film. Based on the above research, due to their excellent mechanical properties, the (AlCrTiZrHf)N high-entropy alloy-nitride films are considered as potential protective surfaces for such kinds of moving parts as gears, cutting tools and shafts used in engines and other mechanical loading components.

5. Conclusions

The (AlCrTiZrHf)N high-entropy alloy-nitride films with different N contents were prepared by reactive magnetron sputtering. The microstructures and mechanical properties of the (AlCrTiZrHf)N high-entropy alloy-nitride films were studied in this paper. The conclusions are drawn as follows:

(1) As the flow rate of N_2 increases, the sputtering rate of the film gradually decreases. The nitrogen content in the high-entropy alloy film first increases rapidly and then stabilizes.
(2) When the N_2 content is 0, the AlCrTiZrHf high-entropy alloy film is amorphous. With the increase of the N_2 flow rate, the crystallinity of the (AlCrTiZrHf)N film is enhanced. The (AlCrTiZrHf)N film is composed of the FCC-structured solid-solution phase.
(3) As the N_2 flow rate increases, the hardness of the (AlCrTiZrHf)N high-entropy alloy film first increases and then slightly decreases, and the friction coefficient of the film first decreases and then increases.
(4) When the N_2:Ar ratio is 5:4, the hardness and elastic modulus of the (AlCrTiZrHf)N film reach the maximum of 33.1 GPa and 347.3 GPa, and the friction coefficient approaches a minimum of 0.5. The strengthening effect is mainly attributed to the formation of saturated metal-nitride phases and the solid-solution strengthening of various elements. Meanwhile, the (AlCrTiZrHf)N film exhibits the low friction coefficient and superior wear resistance.

Declaration of competing interest

The authors declare that they have no known competing financial interests or personal relationships that could have appeared to influence the work reported in this paper.

CRediT authorship contribution statement

Panpan Cui: Writing - original draft. **Wei Li:** Writing - original draft. **Ping Liu:** Formal analysis, Data curation. **Ke Zhang:** Formal analysis, Data curation. **Fengcang Ma:** Formal analysis, Data curation. **Xiaohong Chen:** Formal analysis, Data curation. **Rui Feng:** Formal analysis. **Peter K. Liaw:** Formal analysis.

Acknowledgment

The present work was financially supported by the National Natural Science Foundation of China (No. 51971148, 51471110). P.K.L. thanks the National Science Foundation (DMR-1611180 and 1809640) with program directors, Drs. J. Yang, G. Shiflet, and D. Farkas.

References

[1] J. Piippo, B. Elsener, B.H. Hni, Electrochemical characterization of TiN coatings, Surf. Coating. Technol. 61 (1993) 43–46.
[2] S.H. Ahn, Y.S. Choi, J.G. Kim, J.G. Han, A study on corrosion resistance characteristics of PVD Cr-N coated steels by electrochemical method, Surf. Coating. Technol. 150 (2002) 319–326.
[3] M. Keunecke, C. Stein, K. Bewilogua, W. Koelker, D. Kassel, H. Berg, Modified TiAlN coatings prepared by d.c. pulsed magnetron sputtering, Surf. Coating. Technol. 205 (2010) 1273–1278.
[4] V. Braic, M. Balaceanu, M. Braic, A. Vladescu, S. Panseri, A. Russo, Characterization of multi-principal-element (TiZrNbHfTa)N and (TiZrNbHfTa)C coatings for biomedical applications, J. Mech. Biomed. 10 (2012) 197–205.
[5] W. Li, P. Liu, P.K. Liaw, Microstructures and properties of high-entropy alloy films and coatings: a review, Mater. Res. Lett. 6 (2018) 199–229.
[6] S.Y. Chang, S.Y. Lin, Y.C. Huang, C.L. Wu, Mechanical properties, deformation behaviors and interface adhesion of $(AlCrTaTiZr)N_x$ multi-component coatings, Surf. Coating. Technol. 204 (2010) 3307–3314.
[7] Z.C. Chang, S.C. Liang, S. Han, Y.K. Chen, F.S. Shieu, Characteristics of TiVCrAlZr multi-element nitride films prepared by reactive sputtering, Nucl. Instrum. Methods B. 268 (2010) 2504–2509.
[8] D.C. Tsai, Z.C. Chang, B.H. Kuo, T.N. Lin, M.H. Shiao, F.S. Shieu, Interfacial reactions and characterization of (TiVCrZrHf)N thin films during thermal treatment, Surf. Coating. Technol. 240 (2014) 160–166.
[9] N. Akio, F. Takahiro, M. Toru, Microstructural, mechanical, and corrosion properties of plasma-nitrided CoCrFeMnNi high-entropy alloys, Surf. Coating. Technol. 376 (2019) 52–58.
[10] J.W. Yeh, S.J. Lin, T.S. Chin, J.Y. Gan, S.K. Chen, T.T. Shun, C.H. Tasu, S.Y. Chou, Formation of simple crystal structures in Cu-Co-Ni-Cr-Al-Fe-Ti-V alloys with multiprincipal metallic elements, Metall. Mater. Trans. 35 (2004) 2533–2536.
[11] J.W. Yeh, S.K. Chen, S.J. Lin, J.Y. Gan, T.S. Chin, T.T. Shun, C.H. Tsau, S.Y. Chang, Nanostructured high-entropy alloys with multiple principal elements: novel alloy design concepts and outcomes, Adv. Eng. Mater. 6 (2004) 299–303.
[12] B. Cantor, I.T.H. Chang, P. Knight, A.J.B. Vincent, Microstructural development in equiatomic multicomponent alloys, Mater. Sci. Eng. 375–377 (2004) 213–218.
[13] Y. Zhang, T.T. Zuo, Z. Tang, M.C. Gao, K.A. Dahmen, P.K. Liaw, Z.P. Lu, Microstructures and properties of high-entropy alloys, Prog. Mater. Sci. 61 (2014) 1–93.
[14] D.B. Miracle, O.N. Senkov, A critical review of high entropy alloys and related concepts, Acta Mater. 122 (2017) 448–511.
[15] Y.J. Zhou, Y. Zhang, F.J. Wang, G.L. Chen, Phase transformation induced by lattice distortion in multiprincipal component $CoCrFeNiCuxAl_{1-x}$ solid-solution alloys, Appl. Phys. Lett. 92 (2008) 299.
[16] C.J. Tong, Y.L. Chen, J.W. Yeh, S.J. Lin, S.K. Chen, T.T. Shun, C.H. Tsau, S.Y. Chang, Microstructure characterization of $Al_xCoCrCuFeNi$ high-entropy alloy system with multiprincipal elements, Metall. Mater. Trans. 36 (2005) 881–893.
[17] Y.P. Lu, X.Z. Gao, L. Jiang, Z.N. Chen, T.M. Wang, J.C. Jie, H.J. Kang, Y.B. Zhang, S. Guo, H.H. Ruan, Y.H. Zhao, Z.Q. Cao, T.J. Li, Directly cast bulk eutectic and near-eutectic high entropy alloys with balanced strength and ductility in a wide temperature range, Acta Mater. 124 (2017) 143–150.
[18] Y.P. Lu, Y. Dong, S. Guo, L. Jiang, H.J. Kang, T.M. Wang, B. Wen, Z.J. Wang, J.C. Jie, Z.Q. Cao, H.H. Ruan, Y.H. Zhao, T.J. Li, A promising new class of high-temperature alloys: eutectic high-entropy alloys, Sci. Rep. 4 (2014) 6200.
[19] C.H. Sha, Z.F. Zhou, Z.H. Xie, P. Munroe, FeMnNiCoCr-based high entropy alloy coatings: effect of nitrogen additions on microstructural development, mechanical properties and tribological performance, Appl. Surf. Sci. 507 (2020) 145101.
[20] R. Chen, Z. Cai, J. Pu, Z. Lu, S. Chen, S. Zheng, C. Zeng, Effects of nitriding on the microstructure and properties of VAlTiCrMo high-entropy alloy coatings by sputtering technique, J. Alloys Compd. 827 (2020), 153836.
[21] K. von Fieandt, L. Riekehr, B. Osinger, S. Fritze, E. Lewin, Influence of N content on structure and mechanical properties of multi-component Al-Cr-Nb-Y-Zr based thin films by reactive magnetron sputtering, Surf. Coating. Technol. 389 (2020) 125614.
[22] X.G. Feng, K.F. Zhang, Y.G. Zheng, H. Zhou, Z.H. Wan, Chemical state, structure and mechanical properties of multi-elem ent $(CrTaNbMoV)N_x$ films by reactive magnetron sputtering, Mater. Chem. Phys. 239 (2020) 121991.
[23] S.C. Lin, J. Zhang, R.H. Zhu, S.C. Fu, D.Q. Yun, Effects of sputtering pressure on microstructure and mechanical properties of ZrN films deposited by magnetron sputtering, Mater. Res. Bull. 105 (2018) 231–236.
[24] B. Navinšek, P. Panjan, A. Cvelbar, Characterization of low temperature CrN and TiN (PVD) hard coatings, Surf. Coating. Technol. 74–75 (1995) 155–161.
[25] P. Panjan, I. Bončina, J. Bevk, M. Čekada, PVD hard coatings applied for the wear protection of drawing dies, Surf. Coating. Technol. 200 (2005) 133–136.
[26] L.P. Wang, G.G. Zhang, R.J.K. Wood, S.C. Wang, Q.J. Xue, Fabrication of CrAlN nanocomposite films with high hardness and excellent anti-wear performance for gear application, Surf. Coating. Technol. 204 (2010) 3517–3524.
[27] R.G. Li, S.R. Zhang, C.L. Zou, H.J. Kang, T.M. Wang, The roles of Hf element in optimizing strength, ductility and electrical conductivity of copper alloys, Mater. Sci. Eng. 758 (2019) 130–138.
[28] M.A. Bab, L. Mendoza-Zélis, L.C. Damonte, Nanocrystalline HfN produced by mechanical milling: kinetic aspects, Acta Mater. 49 (2001) 4205–4213.
[29] W.C. Oliver, G.M. Pharr, An improved technique for determining hardness and elastic modulus using load and displacement sensing indentation experiments, J. Mater. Res. 7 (1992) 1564–1583.
[30] K.H. Cheng, C.H. Lai, S.J. Lin, J.W. Yeh, Structural and mechanical properties of multi-element $(AlCrMoTaTiZr)N_x$ coatings by reactive magnetron sputtering, Thin Solid Films 519 (2011) 3185–3190.
[31] C.H. Lai, S.J. Lin, J.W. Yeh, S.Y. Chang, Preparation and characterization of AlCrTaTiZr multi-element nitride coatings, Surf. Coating. Technol. 201 (2006) 3275–3280.
[32] H.W. Chang, P.K. Huang, A. Davison, J.W. Yeh, C.H. Tsau, C.C. Yang, Nitride films deposited from an equimolar Al–Cr–Mo–Si–Ti alloy target by reactive direct current magnetron sputtering, Thin Solid Films 516 (2008) 6402–6408.
[33] R.L. Boxman, V.N. Zhitomirsky, I. Grimberg, L. Rapoport, S. Goldsmith, B.Z. Weiss, Structure and hardness of vacuum arc deposited multi-component nitride coatings of Ti, Zr and Nb, Surf. Coating. Technol. 125 (2000) 257–262.
[34] S.C. Liang, D.C. Tsai, Z.C. Chang, H.S. Sung, Y.C. Lin, Y.J. Yeh, M.J. Deng, F.S. Shieu, Structural and mechanical properties of multi-element (TiVCrZrHf) N coatings by reactive magnetron sputtering, App, Surf. Sci. 258 (2011) 399–403.
[35] T.K. Chen, T.T. Shun, J.W. Yeh, M.S. Wong, Nanostructured nitride films of multi-element high-entropy alloys by reactive DC sputtering, Surf. Coating. Technol. 188 (2005) 193–200.
[36] B. Ren, Z. Shen, Z. Liu, Structure and mechanical properties of multi-element $(AlCrMnMoNiZr)N_x$ coatings by reactive magnetron sputtering, J. Alloys Compd. 560 (2013) 171–176.
[37] S.A. Sharma, Y. Surekha, B. Krishanu, B. Bikramjit, High-entropy alloys and metallic nanocomposites: processing challenges, microstructure development and property enhancement, Mater. Sci. Eng. 131 (2018) 1–42.
[38] K.Y. Tsai, M.H. Tsai, J.W. Yeh, Sluggish diffusion in Co-Cr-Fe-Mn-Ni high-entropy alloys, Acta Mater. 61 (2013) 4887–4897.
[39] Z.C. Chang, S.C. Liang, S. Han, Y.K. Chen, F.S. Shieu, Characteristics of TiVCrAlZr multi-element nitride films prepared by reactive sputtering, Nucl. Instrum. Methods B. 268 (2010) 2504–2509.
[40] C.H. Lai, S.J. Lin, J.W. Yeh, S.Y. Chang, Preparation and characterization of AlCrTaTiZr multi-element nitride coatings, Surf. Coating. Technol. 201 (2006) 3275–3280.
[41] T.K. Chen, T.T. Shun, J.W. Yeh, M.S. Wong, Nanostructured nitride films of multi-element high-entropy alloys by reactive DC sputtering, Surf. Coating. Technol. 200 (2005) 1361–1365.
[42] C.H. Lin, J.G. Duh, J.W. Yeh, Multi-component nitride coatings derived from Ti–Al–Cr–Si–V target in RF magnetron sputter, Surf. Coating. Technol. 201 (2007) 6304–6308.
[43] M.H. Tsai, C.H. Lai, J.W. Yeh, J.Y. Gan, Effects of nitrogen flow ratio on the structure and properties of reactively sputtered $(AlMoNbSiTaTiVZr)N_x$ coatings, J. Phys. D Appl. Phys. 41 (2008) 235402.
[44] P.K. Huang, J.W. Yeh, Effects of nitrogen content on structure and mechanical properties of multi-element (AlCrNbSiTiV)N coating, Surf. Coating. Technol. 203 (2009) 1891–1896.
[45] W.U. Hong, I. Baker, Y. Liu, X.L. Wu, Dry sliding tribological behavior of Zr-based bulk metallic glass, T. Nonferr. Metal. Soc. 22 (2012) 585–589.
[46] S.C. Liang, D.C. Tsai, Z.C. Chang, H.S. Sung, Y.C. Lin, Y.J. Yeh, M.J. Deng, F.S. Shieu, Structural and mechanical properties of multi-element (TiVCrZrHf) N coatings by reactive magnetron sputtering, Appl. Surf. Sci. 258 (2011) 399–403.